We are IntechOpen, the world's leading publisher of Open Access books Built by scientists, for scientists

4,800
Open access books available

122,000
International authors and editors

135M
Downloads

Our authors are among the

154
Countries delivered to

TOP 1%
most cited scientists

12.2%
Contributors from top 500 universities

CLARIVATE ANALYTICS BOOK CITATION INDEX INDEXED

WEB OF SCIENCE™

Selection of our books indexed in the Book Citation Index in Web of Science™ Core Collection (BKCI)

Interested in publishing with us?
Contact book.department@intechopen.com

Numbers displayed above are based on latest data collected.
For more information visit www.intechopen.com

Chapter 8

Bone and Periodontal Tissue Regeneration by the Secretomes from Bone Marrow Derived Mesenchymal Stem Cells

Wataru Katagiri

Additional information is available at the end of the chapter

1. Introduction

Alveolar bone regeneration with grafting is often carried out prior to placement of dental implants. Several graft materials have been used including autogenous bone, xenogeneic bone, and synthetic bone substitutes. Autogenous bone grafts have been used for a long time with good predictability and are considered the "gold standard" because of their osteoinductive and osteoconductive properties and immunogenic compatibility. However, autogenous bone must be harvested from a donor site of the patient and is associated with higher morbidity (Arrington et al., 1996; Joshi et al., 2004). Xenogeneic bone and synthetic bone substitutes such as deproteinized bovine bone, hydroxyapatite, and calcium triphosphate are often used clinically as osteoconductive scaffolds, but they provide limited osteoinductivity and a potential risk of infection and extrusion (Damien et al., 1991). Osteoinductive growth factors such as bone morphogenic protein (BMP)-2 have been used with these osteoconductive materials to promote bone regeneration (Herford & Boyne, 2008). However, recent studies have indicated unexpected effects on bone regeneration including induction of a severe inflammatory response, because of the higher dose with clinical application of BMP-2 (Kawasaki et al., 1998; Perri et al., 2007, Vaidya et al., 2007).

Recently, the concept of tissue engineering and regenerative medicine has been widely accepted (Langer & Vacanti, 1993), and many clinical studies have been performed including studies of bone and periodontal regenerative medicine.

We previously developed a technique whereby autogenous human mesenchymal stem cells (hMSCs) from the patient's bone marrow are combined with platelet-rich plasma for use as an alternative to such materials with predictable good prognosis (Yamada et al., 2004, 2013). However, clinical use of stem cells requires highly qualified safety investigation and quality management of cell handling, and is very expensive. These limitations currently impede the widespread use of stem cells for alveolar bone regeneration therapy. Moreover, recent studies have revealed that the implanted cells do not survive long (Ide et al., 2010; Perri et al., 2007; Toma et al., 2009). As an alternative, the effects of the secretomes, the various factors secreted into the medium, from stem cells on tissue repair and regeneration have attracted much attention (Baglio et al., 2012; Chen et al., 2008; Ciapetti et al., 2012).

We have reported the effects of the secretomes in the conditioned medium from bone marrow-derived mesenchymal stem cells (MSC-CM) on bone and periodontal tissue regeneration *in vitro* and *in vivo*. MSC-CM contains several cytokines such as insulin-like growth factor (IGF)-1, vascular endothelial growth factor (VEGF), and transforming growth factor (TGF)-β1. MSC-CM enhances cell proliferation, mobilization, angiogenesis, and expression of osteogenic markers such as *alkaline phosphatase*, *collagen type I*, and *Runx2* genes (Katagiri et al., 2013). MSC-CM also recruits endogenous stem cells to the grafted site and shows early bone and periodontal regeneration in rat calvarial bone defects and dog periodontal bone defects (Inukai et al., 2013; Osugi et al., 2012). Furthermore, the concentrations of cytokines contained in MSC-CM are relatively low such that use of MSC-CM does not induce the severe histological inflammatory responses that are observed with the clinical use of recombinant human BMP-2 (Katagiri et al., 2013).

In this section, our *in vitro* and *in vivo* studies about the effects of MSC-CM on bone and periodontal tissue regeneration were summarized and introduced.

2. Biological effects of MSC-CM in bore and periodontal tissue regeneration

2.1. Preparation of MSC-CM

The hMSCs were purchased from Lonza and cultured in MSC basal medium (Lonza) with MSC growth medium (SingleQuots, Lonza). Rat MSCs (rMSCs) were isolated from the femora of 7-week-old Wistar/ST rats (Japan SLC) and expanded and cultured in Dulbecco's modified Eagle medium (DMEM) (Gibco) with 10% fetal bovine serum (FBS). Cells of the second to fourth passages were used in the experiments in this study. Cells were maintained at 37°C in 5% carbon dioxide/95% air. The hMSCs were cultured in a culture dish (100 × 20 mm). When hMSCs reached 70% to 80% confluence, the medium was refreshed with 10 mL of serum-free DMEM containing antibiotics (100 units/mL penicillin G, 100 μg/mL streptomycin, and 0.25μg/mL amphotericinB; Gibco). The culture media (CM) was collected after 48 hours of incubation. This media was defined as hMSC culture-conditioned media (MSC-CM) and stored at 4°C or –80°C before being used for subsequent experiments.

Factors	Concentration (pg/mL)
IGF-1	1515.6±211.83
VEGF	465.84±108.81
TGF-β1	339.82±14.41
HGF	20.32±7.89
PDGF-BB	N.D
BMP-2	N.D
FGF-2	N.D
SDF-1	N.D

Table 1. The Levels of Cytokines Present in MSC-CM

2.2. Cytokines present in MSC-CM

The concentrations of the cytokines IGF-1, VEGF, TGF-β1, HGF, FGF-2, PDGF-BB, BMP-2, and SDF-1α in MSC-CM were quantified with ELISA. Cytokines were not detected in DMEM-0% and DMEM-30%. However, MSC-CM contained IGF-1, VEGF, TGF-β1, and HGF at concentrations of 1386 ± 465, 468.5 ± 109, 339.8 ± 14.4, and 20.3 ± 7.8 pg/ml, respectively. The other factors assayed were not detected in MSC-CM (Table 1).

2.3. MSC-CM enhances migration and proliferation of MSCs and PDLCs

The migratory properties of rMSCs and rPDLCs were examined using the CytoSelect Wound Healing Assay kit (Cell Biolabs, San Diego, CA, USA) according to the manufacturer's instructions. Briefly, cell suspension was added to the well with a plastic insert in place. The insert was removed from the well after a monolayer of cells had formed, creating a wound gap of 0.9 mm. After washing, cells were incubated at 37 °C for 48 h in MSC-CM with 30% FBS or serum-free DMEM. The extent of wound closure was determined with a light microscope (CK40; Olympus, Tokyo, Japan) at ×40 magnification. The percentage of rMSCs in the wound area of DMEM (−) was 9.28 ± 4.41. There were 70.9 ± 6.8% rMSCs in the wound area of positive control (30% FBS). MSC-CM exerted significant effects ($p < 0.05$) and closed the wound to 43.4 ± 10.6% rMSCs (Fig. 1a).

The percentage of rPDLCs in the wound area of DMEM (−) was 2.36 ± 2.32%, with 48.01 ± 6.28% in 30% FBS and 17.98 ± 4.14% in MSC-CM. Thus, MSC-CM increased rMSC migration more than four-fold and rPDLC migration more than seven-fold compared with that in DMEM (−). These differences were statistically significant ($p < 0.05$), indicating that MSC-CM enhanced rMSC and rPDLC migration and proliferation (Fig. 1b).

The level of cellular fill within the wound area in response to MSC-CM was compared with the wound-fill response in the presence of 30% FBS or serum-free DMEM as control after 48 h (a). The migration of rMSCs and rPDLSCs cultured in MSC-CM was enhanced compared with

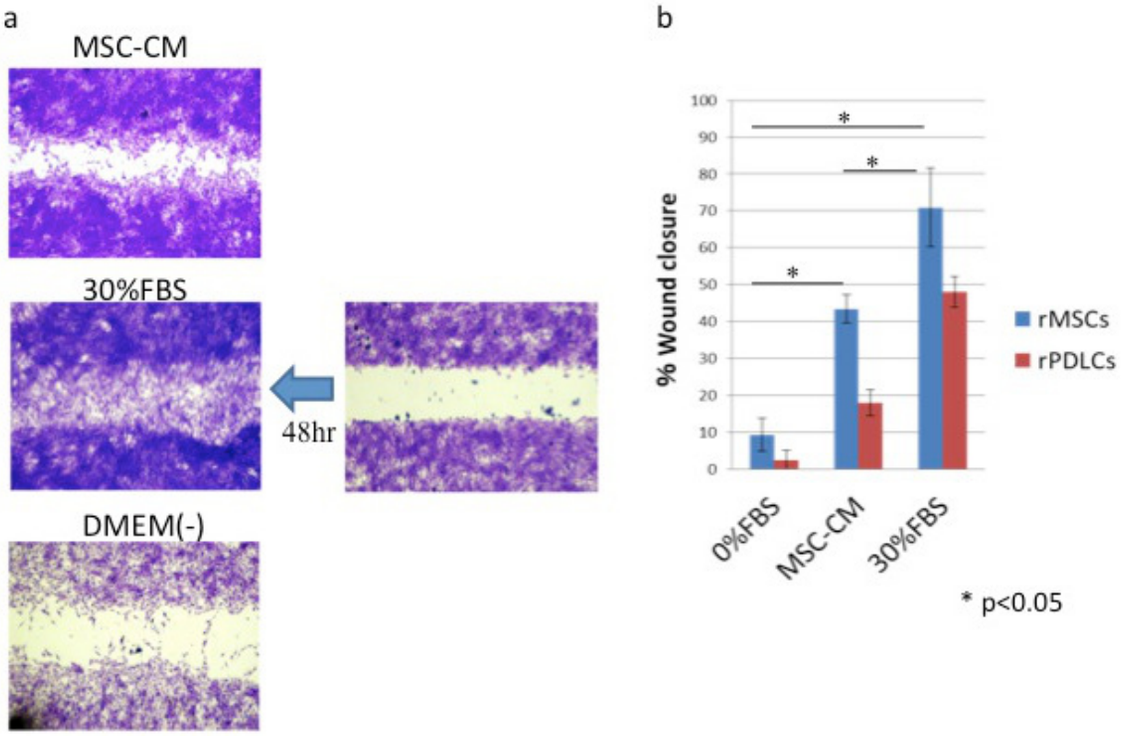

Figure 1. MSC-CM promoted migration and proliferation of rMSCs and rPDLCs in the wound-healing assay.

rMSCs and rPDLSCs cultured in DMEM (−). MSC-CM increased wound area more than 4-fold compared to that in DMEM(-) (b, *$p < 0.05$).

2.4. MSC-CM enhanced MSC migration in rat calvarial bone defect model

rMSCs were harvested and cultured as described previously and were labeled with the lipophilic tracer 1,1-dioctadecyl-3,3,3,3-tetramethylindotricarbocyanine iodide (DiR; Molecular Probes, Eugene, OR) for all imaging ex-periments (Kalchenko et al., 2006). This fluorophore is excited at 750 nm and has an emission peak at 782 nm. The cells were incubated with DiR (3×10^6 cells in 10 mL PBS containing 3.5 mg/mL dye and 0.5% ethanol) for 30 min at 37°C. The cells were then washed twice with PBS and injected intravenously into the caudal vein of Wistar/ST rats with the bone defect de-scribed previously, which had been implanted with vari-ous implant materials just before the injection of rMSCs. The rats were anesthetized by intraperitoneal injection of Somnopentyl® prior to injection. Xenogen's IVIS® 200 Series Imaging System (Xenogen, Alameda, CA) was used to monitor DiR-labeled rMSC localization within live, as well as sacrificed, animals. Imaging was performed at 1, 24, and 48h, and at 1 week after injection of DiR-labeled cells. Migration of rMSCs to the implants in vivo was analyzed in rats of the different implantation groups in which DiR-labeled rMSCs were injected into the caudal vein. Although it is not possible to detect DiR-labeled cells at a great depth with the imaging system used, this system can detect DiR-labeled cells that accumulate on the calvarial bone. The fluorescent signal in all groups increased immediately after injection. In the control Defect group, the fluorescent signal of the labeled rMSCs was only detected in the

tail and abdominal region at 1, 24, and 48 h, and at 1 week after injection. We confirmed that there were no signals at the defect area in the cranium at any time point. In the PBS group, fluorescent signals were observed in the tail and in the abdominal area at 24 and 48h after injection, and very low signals were observed in the breast and cranial area after 1 week. In the MSC-CM group, a moderate increase in signal intensity was observed in the area of the tail and the abdominal region during the first 24h after injection. At 48h after injection, signal intensity in the MSC-CM-implanted area of the parietal bone started to increase. The maximum fluorescent signal in the implanted area was observed 1 week after injection (Fig. 2).

In vivo imaging analysis shows that DiR-labeled rMSCs that were injected into the caudal vein just after implantation of the materials into the calvarial bone defects started to mi-grate immediately after injection. At 24 h, 48 h, 72h and 1 week after injection, the signal of the fluorescent-labeled rMSCs was only detected in the tail and abdominal region in the control PBS group. In the MSC-CM group, a moderate increase in signal intensity was observed in the abdominal region during the first 24 h after injection. Forty-eight hours after injection, the MSC-CM-implanted area of calvarial bone started to increase in signal intensity, and, 1 week after injection, the MSC-CM implanted area, as well as the implanted bone cavity, showed the highest fluorescent signal of the experimental groups.

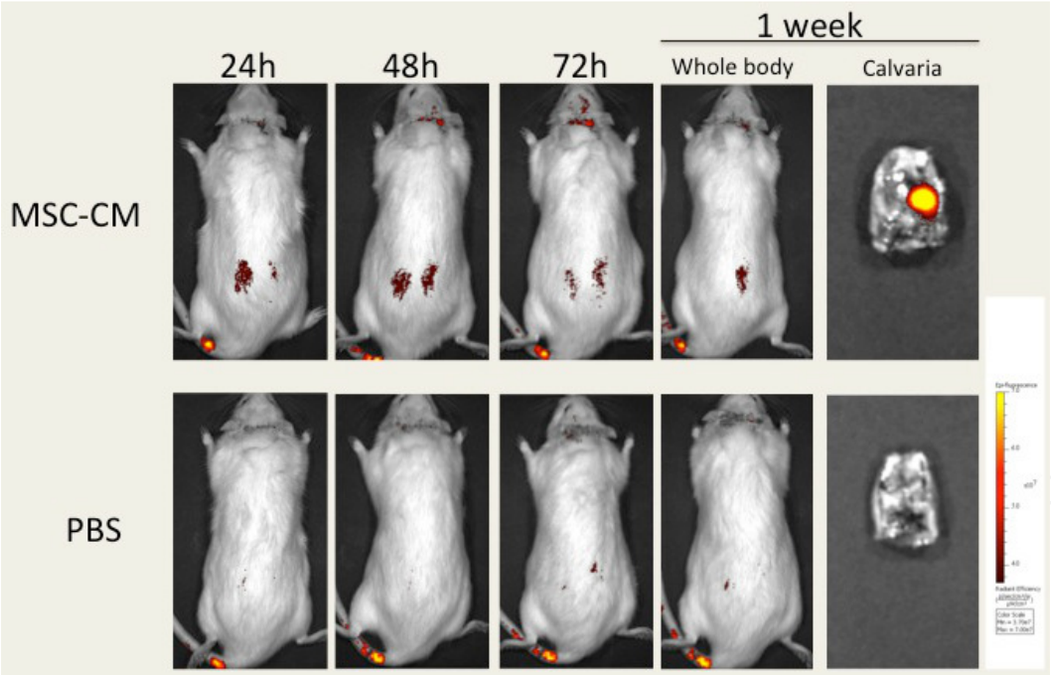

Figure 2. In vivo imaging of injected rMSC migration to implants.

2.5. MSC-CM enhanced osteogenic and angiogenic marker gene expression

The levels of expression of the *ALP*, *OCN*, *Runx2*, *VEGF-A*, *ANG-1*, and *ANG-2* genes were significantly upregulated in rMSCs cultured with MSC-CM compared with rMSCs cultured in EM (Fig. 3).

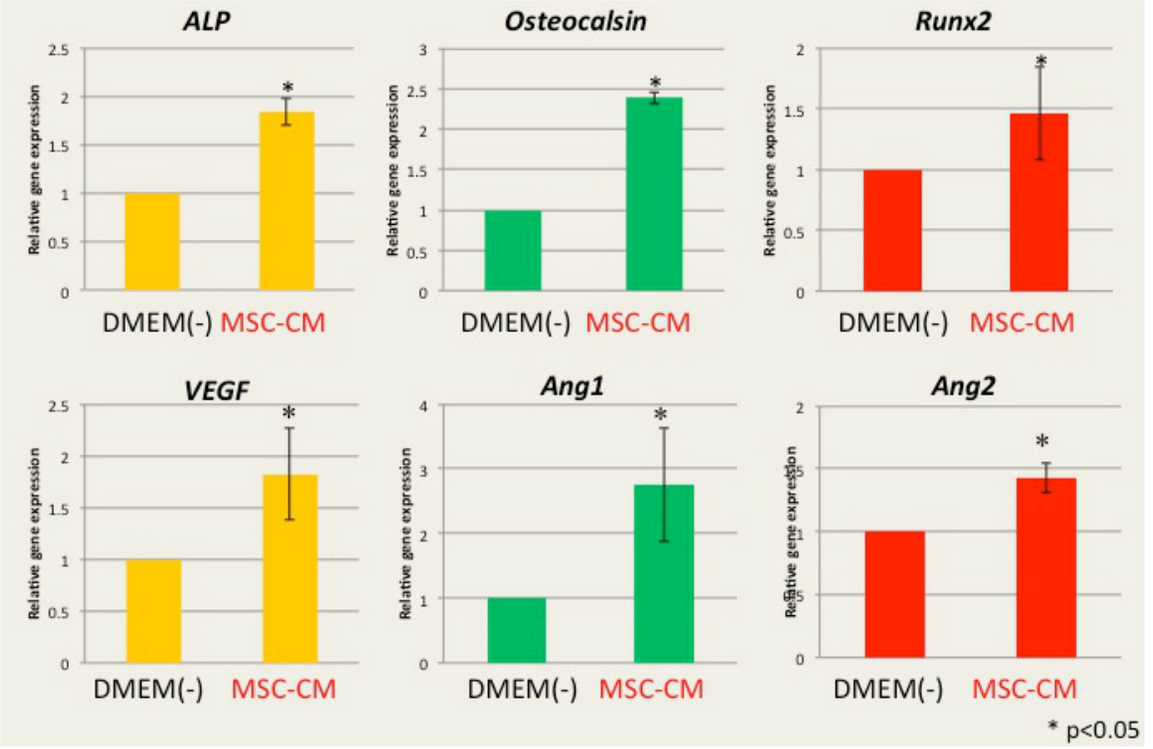

Figure 3. MSC-CM enhanced osteogenic and angiogenic marker gene expression.

The mRNA expression levels of *ALP*, *OCN*, *Runx2*, *VEGF-A*, *ANG-1*, and *ANG-2* were determined relative to the level of *Glyceraldehyde 3-phosphate dehydrogenase* (*GAPDH*) mRNA in each sample and were quantified and standardized. The level of expression of the each gene was significantly upregulated in rMSCs cultured with MSC-CM compared with rMSCs cultured in DMEM (*$p < 0.05$).

2.6. MSC-CM enhanced bone regeneration, migration of endogeneous MSCs and angiogenesis in rat calvarial bone defect model

Twenty-four 10-week-old male Wistar/ST rats were anesthetized by intraperitoneal injection of pento-barbital (Somnopentyl, Kyoritsu Seiyaku) (20 mg/kg body weight). Two circular full-thickness (through-and-through) bone defects (5 mm in diameter) were made in the calvarial bone using a trephine bur and were irrigated with saline to remove the bone debris. The experimental materials were then implanted into the defects. Atelocollagen (Terudermis, Olympus Terumo Biomaterials), which was cut into the desired form, was suspended in MSC-CM or PBS. Three groups were de-fined: *(1)* MSC-CM group: MSC-CM/Terudermis; *(2)* PBS group: PBS/Terudermis; and *(3)* defect group: unfilled defect.

Rats were sacrificed at 2 or 4 weeks after transplantation (n=4 per group). The surgical sites were dissected, fixed in 10% formalin, and subjected to micro-computed tomography (micro-CT) analysis using a laboratory x-ray CT device (LATheta, Hitachi Aloka). Images were compiled and analyzed to render three-dimensional images using OsiriX imaging software (version 3.9). Then the area (mm^2) of newly regenerated bone was compared between groups.

The explants were decalci-fied with K-CX solution (FALMA) and dehydrated using a graded series of ethanols, cleared with xylene, and embedded in paraffin. The specimens were cut in a sagittal direction to make 3-μm-thick histologic sections and stained with hematoxylin-eosin. Histologic analysis was performed using a light microscope. MSC-CM/Terudermis or control implants were placed into rat calvarial bone defects (Fig 4a). The area of newly regenerated bone was determined as a percentage of the total graft area at 2 and 4 weeks post-implantation using micro-CT (Fig 4b). After 2 weeks, the mean area of newly regenerated bone in the MSC-CM defects (81.50% ± 2.7%) was significantly increased compared to that of the unfilled defects (8.63% ± 1.78%) and the PBS-treated sites (60.63% ± 5.8%). After 4 weeks, the defect areas were almost completely filled by newly regenerated bone in the MSC-CM (93.07% ± 6.6%) and PBS (84.04% ± 4.9%) groups (Fig 4b). Moreover, histologic analysis also showed well-regenerated bone in the MSC-CM group compared with the PBS groups (Fig 5). At 2 weeks, the bone defect was almost covered with newly regenerated bone in the MSC-CM group, in contrast to the PBS group, where the defect was covered with a large amount of connective tissue. At 4 weeks, newly regenerated bone was partially noticeable within the defect of the PBS group, but in the MSC-CM group, the defect was almost completely replaced by mature bone tissue (Fig 5).

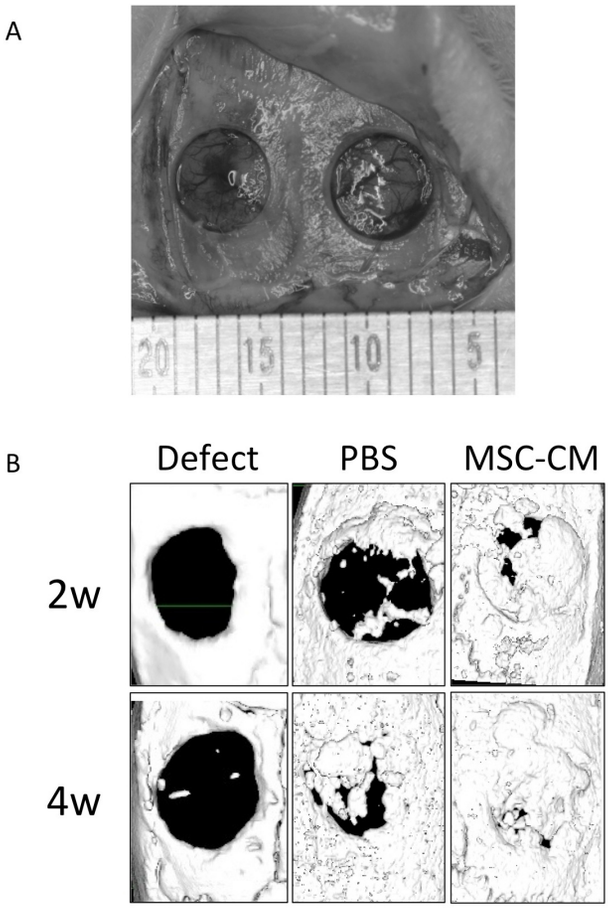

Figure 4. (a) Bone defect 5mm in diameter was prepared in each rat calvaria. (b) Micro-CT analysis of bone regeneration.

Images of micro-CT indicated that the newly regenerated bone was seen at an early stage of bone regeneration and almost covered the defect at 4 weeks. (c) Percent bone regeneration by area within defects as measured by micro-CT at 2 and 4 weeks. MSC-CM increased the bone regeneration significantly compared with other groups at 2 and 4 weeks (*p<0.01, #p<0.05).

Furethermore, we performed the immunohistochemical staining against CD31 and CD105 antibody to confirm the endogeneous MSC migration and angiogenesis during the bone regeneration by MSC-CM. In the MSC-CM group, numerous CD31-or CD105--positive cells were seen the MSC-CM implanted area. In contrast, there were fewer CD31-or CD105-positive cells in both the PBS and Defect groups (Fig 6). These results indicated MSC-CM enhanced the endogeneous MSC migration and angiogenesis.

Newly regenerated bone in the defect, PBS and MSC-CM groups 2 or 4 weeks after implantation was evaluated. In the defect group, majority of the defect was filled with connectivetissue and the infiltrations of inflammatory cells were seen both at 2 and 4 weeks. In the MSC-CM group, newly regenerated bone had begun to cover the defect at 2 weeks and ossification had progressed gradually. In the PBS group, newly regenerated bone and partial connective tissue had covered the defect at 4 weeks.

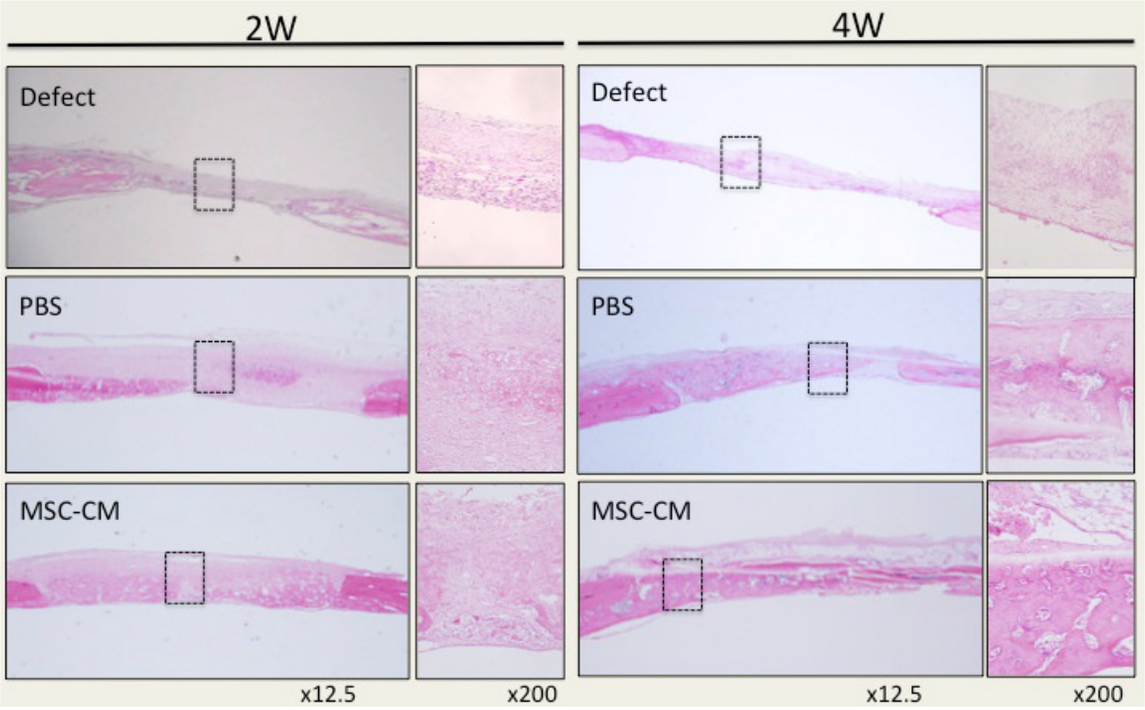

Figure 5. Histological analysis of newly regenerated bone.

Two weeks after implantation into carvalial defects, tissue specimens were analyzed using immunohistostaining for: CD31 (RED), a marker for rat endothelial cells; CD105 (GREEN), a marker for rat stem cells. Cell nuclei were labeled with DAPI (blue). In MSC-CM group, both CD105 and CD31 positive cells were more prominent than those of the control PBS group.

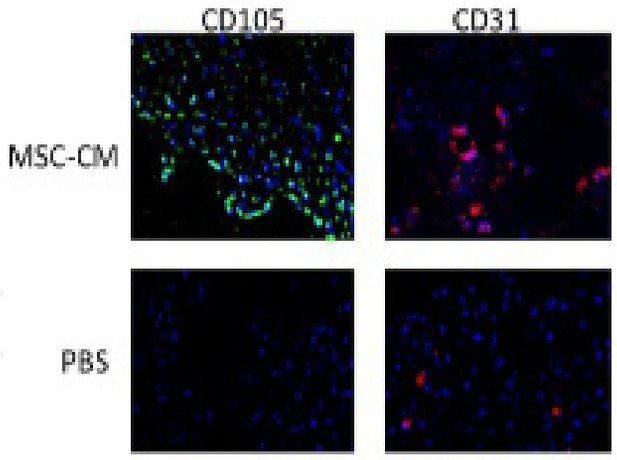

Figure 6. Immunohistochemical analysis of newly generated bone area 2 weeks after implantation.

2.7. MSC–CM enhanced periodontal tissue regeneration in dog periodontal defect model

All animal experiments were approved by the Nagoya University animal experiment committee. After a period of acclimatization of 30 days, five hybrid dogs were operated on under general anesthesia by intravenous injection of pentobarbital (Somnopentyl®) (20mg/kg body weight), and under local anesthesia with 2% lidocaine (with 1:80,000 epinephrine, ORA® Inj. Dental Cartridge; Showa Yakuhin Kako, Tokyo, Japan). Before the experimental surgery, the mandibular first and third or fourth premolars were extracted, and the extraction sites were allowed to heal for 8 weeks. For the experimental surgery, buccal and lingual mucoperiosteal flaps were elevated, and critical-size, box-type, one-wall intrabony defects (width, 4mm; height, 5 mm) were created at the distal aspect of the second, and the mesial aspect of the fourth premolars in the right and left jaw quadrants (Kim, 2005). Following root planing to remove the root cementum, a reference notch indicating a 5-mm distance from the cement-enamel junction to the bottom of the defect was made with a burr into the root surface at the base of the defects. With no differences in bone regeneration in the various grafted areas in terms of bone healing, two defects were created and implanted with two materials at random sites. An absorbable atelo-collagen sponge (TERUPLUG®; OLYMPUS TERUMO BIOMATERIALS, Tokyo, Japan) was used as a scaffold and contained 300μl MSC-CM or PBS. The dogs with defects were randomly divided into three groups (n=6 each) and implanted with graft materials: MSC-CM plus scaffold, PBS plus scaffold, or unfilled defect. The mucogingival flaps were advanced, adapted, and completely closed. Post-surgical management involved antibiotics (Azithromycin, 250 mg; Pfizer, Tokyo, Japan) daily for 3 days, a soft diet, and topical application of 2% chlorhexidine (Hibitane concentrate; Dainippon Sumitomo Pharma, Osaka, Japan) twice a week. After 4 weeks, the dogs were given general anesthesia and sacrificed by exsanguination after injection of heparin sodium (400 U/kg).

Standardized radiographic images of the defect sites were obtained with an X-ray apparatus (Dent navi Hands; Yoshida Co., Ltd., Tokyo, Japan) and dental X-ray films (BW-100; Hanshin Technical Laboratory, Nishinomiya, Japan) immediately, and 4 weeks after, transplantation.

Dental X-ray films were placed parallel to the tooth axis, and radiographic images of the defect site were ta-ken in the buccolingual direction. The defect sites were dissected and fixed in 10% neutral-buffered formalin (Wako, Japan) 4 weeks after transplantation. The specimens were decalcified in Plank-Rychro solution (Wako) for 8 weeks, routinely processed into 5μm-thick paraffin-embedded sections, stained with hematoxylin and eosin, and observed under a light microscope (Olympus). Histometric parameters were quantified using a computer-based image analysis system (Image J 1.44; National Institutes of Health). The following parameters were analyzed:

1. Cementum regeneration height: distance from the root surface notch to the coronal extension of newly formed cementum on the root surface.

2. Bone regeneration height: distance from the root surface notch to the coronal extension of newly formed bone along the root surface.

3. Bone regeneration area: area of new alveolar bone formed coronally from the apical extension of the root surface notch.

Clinical healing was generally uneventful. The results from the histometric analysis are shown in Fig. 8. The cementum regeneration height, the bone regeneration height, and the bone regeneration area of the MSC-CM group were 3.01 ± 0.16 mm, 3.19 ± 0.51 mm, and 4.89 ± 1.08 mm^2, respectively. A large amount of new lamellar and woven bone formation was observed in the MSC-CM group. Thick-layered and cellular cementum on the root surface was also frequently observed in the MSC-CM group.

On the other hand, less newly regenerated bone and cementum compared to the MSC-CM group was observed in the PBS group. Dense collagen fibers were observed frequently in the PBS group. Newly regenerated bone and cementum were not apparent in the defect group. Furthermore, there was minimal inflammatory cell infiltration in the MSC-CM group compared to the other groups.

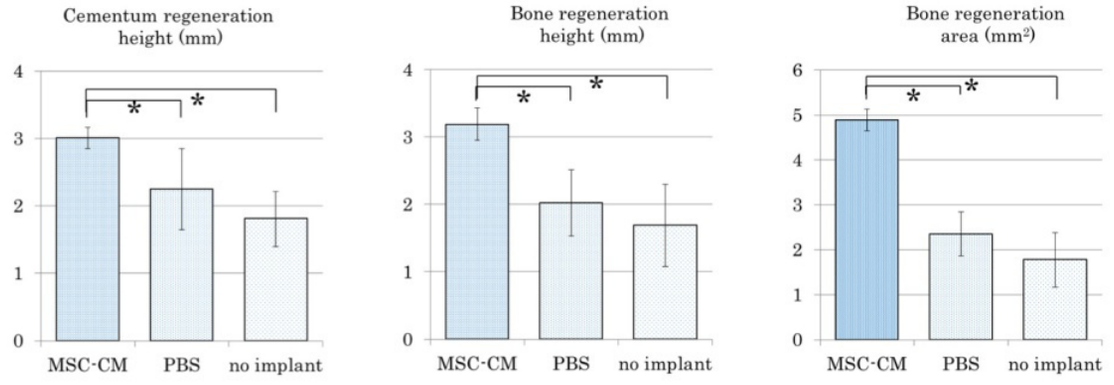

Figure 7. Representative photomicrographs and radiographic images from sites receiving experimental materials.

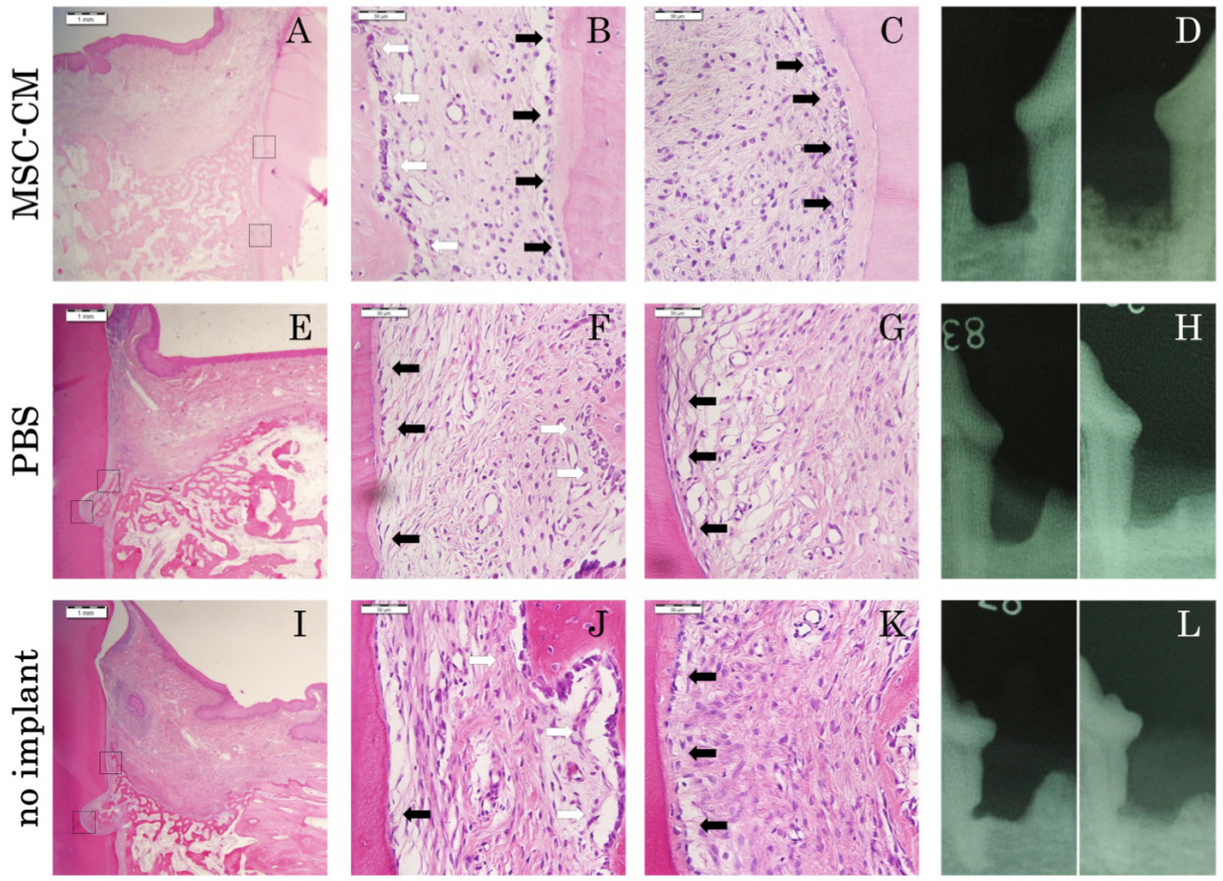

White arrows: osteoblasts. Black arrows: newly regenerated cellular cementum. Photomicrographs: hematoxylin and eosin staining.

Figure 8. (A, E and I) overview of periodontal defect site. Original magnification x12.5, scale bar=1 mm. (B, C, F, G, J and K) Higher magnification of the boxed areas. Original magnification x100, scale bar=50 lm. (D, H and L) Radiographic images were taken at 0 (left) and 4 weeks (right) after surgery. Histometric analysis of periodontal regeneration following surgical implantation of MSC-CM/TERUPLUG® in dog one-wall intrabony defects (means ± SD in mm or mm^2) ($p < 0.05$).

3. Conclusion

From the results of these studies, it was suggested that MSC-CM contributes to upregulation of several processes of bone and periodontal tissue regeneration through the angiogenesis and mobilization of endogenous MSCs, and thus enhanced bone and periodontal tissue regeneration. Using MSC-CM for bone and periodontal tissue regeneration may be effective because several cytokines, including MSC-CM, contribute several processes to the complex system of bone and periodontal tissue regeneration. If the MSC-CM treatment protocol is to be established for bone and periodontal tissue regeneration, it is essential that effective and therapeutic doses of MSC-CM as well as the safety of the therapy should be carefully established. Further investigation regarding these matters is now in progress.

Author details

Wataru Katagiri

Nagoya University Graduate School of Medicine, Japan

References

[1] Arrington ED, Smith WJ, Chambers HG, Bucknell AL & Davino NA. (1996). Complications of iliac crest bone graft harvesting. *Clin Orthop Relat Res,* Vol.329, (August 1996), pp.300-309, ISSN 0009-921X.

[2] Baglio SR, Pegtel DM & Baldini N. (2012). Mesenchymal stem cell secreted vesicles provide novel opportunities in (stem) cell-free therapy. *Front Physiol* Vol 3, (September 2012), pp.1-11, ISSN 1664-042X.

[3] Chen L, Tredget EE, Wu PYG & Wu Y. (2008). Paracrine factors of mesenchymal stem cells recruit macrophages and endothelial lineage cells and enhance wound healing. *PloS ONE*, Vol. 3, No.4, (June 2008), pp.e1886, ISSN 1932-6203.

[4] Ciapetti G, Granchi D & Baldini N. (2012). The combined use of mesenchymal stromal cells and scaffolds for bone repair. *Curr Pharm Des*, *Vol.* 18, No.13, (July 2012), pp. 1796–1820, ISSN 1873-4276.

[5] Damien CJ & Parsons JR. (1991). Bone graft and bone graft substitutes: a review of current technology and applications. *J Appl Biomater* Vol. 2, No.3, (June 1996), pp. 187-208, ISSN 1045-4861.

[6] Herford AS & Boyne PJ. (2008), Reconstruction of mandibular continuity defects with bone morphogenic protein-2 (rhBMP-2). *J Oral Maxillofac Surg,* Vol.66, No.4, (April 2008), pp.616-624, ISSN 1531-5053.

[7] Ide C, Nakai Y, Nakano N, Seo T, Yamada Y, Endo K, Noda T, Saito F, Suzuki Y, Fukushima M & Nakatani T. (2010). Bone marrow stromal cell transplantation for treatment of sub-acute spinal cord injury in rat. *Brain Res,* Vol.1332, (May 2010), pp.32-47, ISSN 1872-6240.

[8] Inukai T, Katagiri W, Yoshimi R, Osugi M, Kawai T, Hibi H & Ueda M. (2013). Novel application of stem cell-derived factors for periodontal regeneration. *Biochem Biophys Res Commun*, Vol.430, No. 2, (January 2013), pp.763-768, ISSN 1090-2104.

[9] Joshi A & Kostakis GC. (2004). An investigation of post-operative morbidity following iliac crest graft harvesting. *Br Dent J,* Vol.196, No. 3, (March 2004), pp.167-171, ISSN 0007-0610.

[10] Kalchenko V, Shivtiel S, Malina V, Lapid K, Haramati S, Lapidot T, Brill A, & Harmelin A. (2006). Use of lipophilic near-infrared dye in whole-body optical imaging of

hema-topoietic cell homing. *J Biomed Opt Vol.* 11, No.5, (January 2007), pp.50507, ISSN 1083-3668.

[11] Katagiri W, Osugi M, Kawai T & Ueda M. (2013). Novel cell-free regenerative medicine of bone using stem cell derived factors. *Int J Oral Maxillofac Implants* Vol. 28, No. 4, (March 2014), pp.1009-1016, ISSN 1942-4434.

[12] Kawasaki K, Aihara M, Honmo J, Sakurai S, Fujimaki Y, Sakamoto K, Fujimaki E, Wozney JM & Yamaguchi A. (1998). Effects of reconmbinant human bone morphogenetic protein-2 on differentiation of cells isolated from human bone, muscle, and skin. Bone 1998: 23, No.3, (December 1998), pp223-231, ISSN 8756-3282.

[13] Kim CS, Choi SH, Cho KS, Chai JK, Wikesjö UM & Kim CK. (2005). Periodontal healing in one-wall intra-bony defects in dogs following implantation of autogenous bone or a coral-derived biomaterial. *J Clin Periodontol*, Vol.32, No.6, (January 2005), pp.583–589, ISSN 0303-6979.

[14] Langer R & Vacanti JP. (1993). Tissue engineering. *Science*, Vol.260, No.5110, (June 1993), pp.920-926, ISSN 0036-8075.

[15] Osugi M, Katagiri W, Yoshimi R, Inukai T, Hibi H & Ueda M. (2012). Conditioned media from mesenchymal stem cells enhancedbone regeneration in rat calvarial bone defects. *Tissue Eng Part A*, Vol. 18, No. 13-14, (July 2012), pp.14779-1489, ISSN 1937-335X.

[16] Perri B, Cooper M, Lauryssen C & Anand N. (2007). Adverse swelling associated with use of rh-BMP-2 in anterior cervical discectomy and fusion: a case study. *Spine J*, Vol. 7, No.2, (May 2007), pp.235-239, ISSN 1529-9430.

[17] Toma C, Wagner WR, Bowry S, Schwartz A & Villanueva F. (2009). Fate of culture-expanded mesenchymal stem cells in the microvasculature: in vivo observations of cell kinetics. *Circ Res*, Vol.104, No.3, (February 2009), pp.398-402, ISSN 1524-4571.

[18] Vaidya R, Carp J, Sethi A, Bartol S, Craig J & Les CM. (2007). Complications of anterior cervical discectomy and fusion using recombinant human bone morphogenetic protein-2. *Eur Spine J,* Vol.16, No.8, (November 2007), pp.1257-1265, ISSN 0940-6719.

[19] Yamada Y, Ueda M, Naiki T, Takahashi M, Hata K & Nagasaka T. (2004). Autogenous injectable bone for regeneration with mesenchymal stem cells (MSCs) and platelet-rich plasma (PRP) – Tissue-engineered bone regeneration. T*issue Eng,* Vol.10, No.5-6, (January 2005), pp.955-964, ISSN 1076-3279.

[20] Yamada Y, Nakamura S, Ito K, Umemura E, Hara K, Nagasaka T, Abe A, Baba S, Furuichi Y, Izumi Y, Klein OD & Wakabayashi T. (2013). Injectable bonetissue engineeringusingexpanded mesenchymal stem cells. *Stem Cells*, Vol.31, No.3, pp.572-580, ISSN 1549-4981.

IntechOpen